PREPARATION OF METAL ORGANIC FRAMEWORK (MOF) DERIVED BIMETALLIC CATALYST FOR DRY REFORMING OF METHANE

Kah Chun Chin[1], Loong Kong Leong[1*], Shih-Yuan Lu[2], De-Hao Tsai[2], Sumathi a/p Sethupathi[3]

[1]*Department of Chemical Engineering, University Tunku Abdul Rahman (UTAR), Bandar Sungai Long, 43000, Kajang, Selangor, Malaysia.*
[2]*Department of Chemical Engineering, National Tsing Hua University (NTHU), 30013, Hsinchu, Taiwan, R.O.C*
[3]*Department of Environmental Engineering, University Tunku Abdul Rahman (UTAR), Bandar Barat, 31900, Kampar, Perak, Malaysia.*

ABSTRACT

In the past decade, efforts have been focused on development of catalyst to show high activity for dry reforming of methane (DRM). The development of catalyst has been crucial to be carried out as this may significantly reduce the concentration of most common greenhouse gases, namely methane (CH_4) and carbon dioxide (CO_2) in the atmosphere. In present work, a series of varying molar ratio of Ni:Ce metal organic framework (MOF) derived catalysts were grown on alumina in one step. The synthesis steps were in accordance to reported solvothermal method for the syntheses of NH_2-MIL-88B with slight modification. This was followed by reduction at 500°C in hydrogen environment for 1 h. The physical and chemical properties of the catalysts were probed by powder XRD, BET surface area analysis, EDX, ICP, CO_2-TPD and H_2-TPR. XRD showed that diffraction patterns were in agreement with the diffraction pattern of MOF synthesized in previous work, thus confirmed the successful formation of the MOF structure. The variation in the molar ratio of Ni:Ce did not show significant difference in the diffraction pattern of the MOF-derived catalysts. For reduction phase, sharp diffraction peaks were detected at $2\theta = 44.5°$, $51.85°$, and $76.37°$, which can be indexed to (1 1 1), (2 0 0) and (2 2 0) planes of face-centered cubic (FCC) metallic Ni, respectively. The addition of Ce promoted smaller particle size of Ni, ranging from 4.6 nm to 6.88 nm. The presence of CeO_2 was observed at $2\theta = 28.6°$, $33.0°$, and $56.4°$. Elemental distribution was compared between EDX and ICP-OES. ICP-OES and EDX analyses indicated that weight percent of bimetallic metal of Ni and Ce was consistent, in which the amount of respective metal obeyed the ratio trend of the metal precursors added during the MOF synthesis. This suggested the homogeneity of the catalyst, even though EDX showed relatively higher weight percent than ICP-OES. The catalytic performance of catalysts showed that 1Ni1Ce exhibited better conversion of CH_4 and CO_2, with 63.5% and 86.8% respectively at 800ºC, and the conversion tend to increase at a higher temperature. The results were convincing for the design of a performing catalyst for DRM process.

Keywords: Alumina support; Dry reforming of methane; Metal organic framework; Nickel-cerium

*Corresponding author's email: leonglk@utar.edu.my, Tel. +603-9086-0288, Fax. +603-9019-8868

1.   INTRODUCTION

Based on the 2013 Intergovernmental Panel on Climate Change (IPCC) report, anthropogenic greenhouse gases, namely GHG emissions since the early Industrial Revolution, have led to global warming of 1.0°C (Anderson et al., 2016). The evidence and statistics show that GHG emissions are strongly related to observable effects on global warming (Solomon et al., 2017). CO_2 and CH_4 were reported to be the most common GHG in Earth's atmosphere, in terms of emission quantity and total impact on the global warming (Smith et al., 2013). Hence, it is crucial to develop method to mitigate this problem, as both the concentration of GHGs and warming rates are expected to increase drastically in the future. Rather than capturing CO_2 and CH_4, the consumption of two natural abundant GHGs is undoubtedly an attractive route to reduce the GHG in an environmental-friendly way. In this regard, dry reforming of methane (DRM) was introduced by reacting both GHGs, forming a mixture of hydrogen (H_2) and carbon monoxide (CO) generally known as syngas (Winanti et al., 2014). This is a feasible way to reduce GHGs without complicated and expensive separation process (San-José-Alonso et al., 2009; Rubin et al., 2015). Furthermore, low CO/H_2 ratio associated with syngas from DRM is necessary for certain downstream applications, such as Fischer Tropsch process and synthesis of oxygenated materials (Tristantini Budi et al., 2015; Nataj et al., 2019).

In the past decade, well-documented literature has been focused on development of high activity and stability catalyst for DRM. In summary, transition metal (e.g., Ni, Co and Fe) and noble metal (Rh, Pt) were found to have a promising catalytic performance in terms of conversion and selectivity for reactants (Pakhare & Spivey, 2014). Due to its wide availability and low cost, alumina-supported Ni catalysts were most widely used in large-scale industrial contexts (Souza et al., 2004). However, the process of rapid catalyst deactivation by sintering and poisoning via coke formation is still a serious concern for Ni metal-based catalyst (Kim et al., 2016).

As a result, this work has focused on the use of perovskite-liked material, such as metal-organic framework (MOF). Composed of geometrically well-defined structures of central metal atoms connected by organic linkers, the MOF can be used as a structure-by-design precursor to produce highly-dispersed metallic particles (Rogge et al., 2017). The additional of CeO_2 promotes higher activity with more stable basic sites, and inhibits the coke deposition due to its high oxygen mobility, high oxygen storage capacity and constraint on particle size, as reported in previous literature (Loc et al., 2017; Movasati et al., 2017)

In this study, a facile approach focused on the effects of Ni:Ce molar ratio on catalytic performance of an alumina-supported catalyst in DRM. A series of bimetallic catalysts with various Ni/Ce ratios were prepared through solvothermal method, and characterized to study the physical and chemical properties of the MOF-derived catalysts. A catalytic test was carried out, ranging from 300 to 900°C in order to evaluate their activity and stability of MOF-derived catalysts. To our knowledge, there is no literature data about the derivation of DRM catalyst for MOF precursor.

2.   RESEARCH METHODOLOGY

2.1. Catalyst Preparation

The MOF-derived catalyst was supported with alumina in one step by following the reported solvothermal method for NH_2-MIL-88B with slight modification. Typically, a reaction mixture containing 4.5 mmol of H_2N-BDC ($\geq$ 99%. Alfa Aesar) with varying molar ratio of $Ni(NO_3)_2.6H_2O$ ($\geq$ 99.9%, Merck) and $Ce(NO_3)_3.6H_2O$ ($\geq$ 99.9%, Merck) and 1g of γ-Al_2O_3 ($\geq$ 99.9%, Merck) was stirred in 50 mL of DMF ($\geq$ 99.8%, Acros Organic). The Ni:Ce precursor molar ratio was controlled in successive value, being 1:1, 2:1, 1:2, with total molar ratio of 4.5

mmol. The resulting solution was then transferred to a 100 mL Teflon liner, followed by addition of 0.75 mL of acetic acid (≥99.8%, Sigma Aldrich) and ultrasonic treatment in order to ensure homogenous mixing. The Teflon liner was transferred into an autoclave and crystallized for 10 h at 125°C. The resulting product was recovered and washed with DMF, deionized water, and ethanol sequentially by centrifugation to remove the surfactant and excessive reactants. The samples were then vacuum dried at 80°C for later use. The catalysts were denoted as following aNibCe, in which a and b interpreted the molar ratio of respective elements.

2.2. Characterization

The crystalline structure of the prepared catalysts was investigated by Bruker 2D Phaser XRD with CuKα radiation (λ = 0.15406 nm) varying 2θ in the range of 10-80°. The elemental composition of catalysts was investigated with ICP-OES (Perkin Elmer, Optima 7000) and SEM-EDX (Hitachi, S-3400N). A Brunauer-Emmett-Teller (BET) surface area analysis was carried out to study specific surface area and porosity of the catalysts. The samples were degassed for 3 h at 150°C before measurements were taken by means of Micromeritics ASAP 2020 to remove moisture and other adsorbed gases from the catalyst surface. Temperature programmed reduction (H_2-TPR) and desorption (CO_2-TPD) was carried out with TPDRO1100 (Thermo Scientific). H_2-TPR explained the reducibility of active Ni species and interaction between nickel species and γ-Al_2O_3 support, while the CO_2-TPD studied the basicity of catalyst. For H_2-TPR, the prepared sample was pretreated with N_2 for 1 h at 500°C and then cooled to 200°C. Subsequently, the analysis was carried out in a mixture 5.55% H_2 /N_2 with a heating rate of 10°C/min to 1000°C. CO_2-TPD was performed the by reducing the sample in a mixture of 5.55% H_2 /N_2 for 1 h at 500°C. The sample was cooled room temperature and saturated under pure CO_2 stream for 30 minutes. The subsequent analysis was carried out in an He environment by heating the sample with a heating rate of 10°C/min to 900°C.

2.3. Catalytic Test

Catalytic activity measurements of the catalysts were performed in a U-shaped fixed-bed quartz tube reactor. Prior the reaction, the catalyst was loaded in the tube furnace and reduced in pure H_2 at 500°C for 1 hour to activate the catalyst. 200 mg of reduced sample were then loaded into the reactor and a mixture of equimolar CH_4/CO_2 was passed through the catalyst, which was then mixed with internal standard gas of N_2. Quartz wool was used to hold the catalyst bed in a fixed position. Catalytic performance was evaluated from 300−900°C.

3. RESULTS AND DISCUSSION

3.1. Catalyst Characterization

Figure 1a shows crystalline structure of MOF-derived catalysts before reduction. In agreement with the diffraction pattern of NiMOF synthesized in previous work, the results confirm successful formation of an MOF structure (Senthil Raja et al., 2018). It should be noted that the variation in the molar ratio of Ni:Ce does not show significant difference in the diffraction pattern of MOF catalysts. XRD patterns of reduced sample are presented in Figure 1b. One can assert that peak characterizing phase at 2θ = 37.6°, 45.9°, and 67.0° in all catalysts [JCPDS No. 10-0425] indicates the presence of γ-Al_2O_3 as support for catalytic application. For the reduced sample, the characteristic peaks of CeO_2 were positioned at 2θ = 28.6°, 33.0°, and 56.4° [JCPDS No. 34-0394], with active Ni at 2θ = 44.5°, 51.85°, and 76.37° [JCPDS No. 04-0850], corresponding to (1 1 1), (2 0 0) and (2 2 0), respectively. The presence of CeO_2 could inhibit catalyst from forming $NiAl_2O_4$ at 2θ = 19.0° and 46.0°, which could deteriorate the catalyst's activity (Loc et al., 2017).
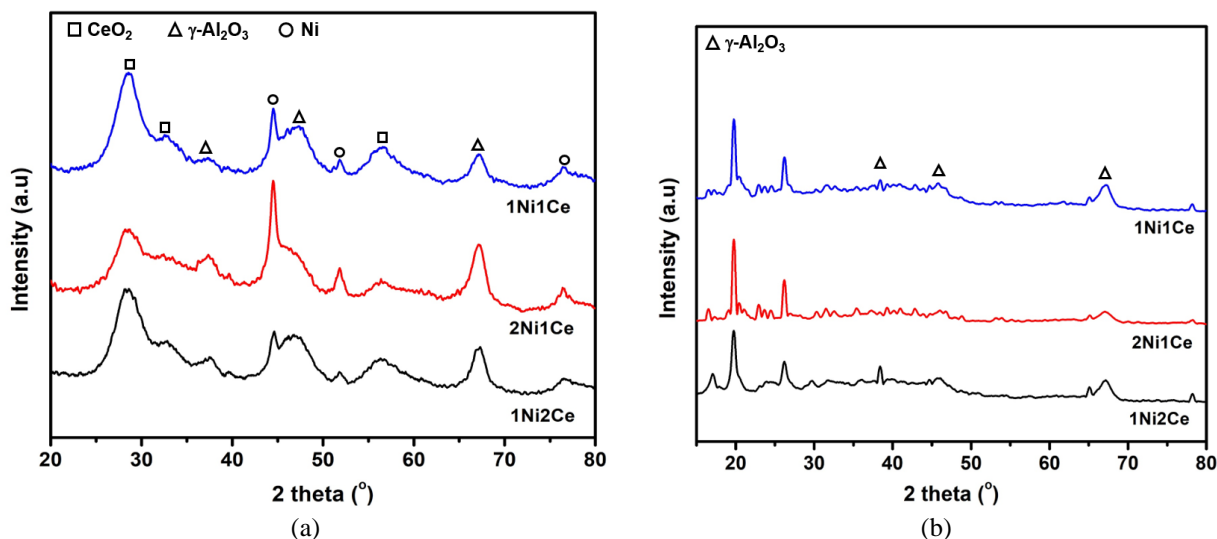
(a)   (b)

Figure 1 XRD patterns of supported MOF-derived catalyst: (a) before; and (b) after reduction

The specific surface area and average pore diameter of MOF derived catalysts were characterized. Figure 2a shows that all catalysts displayed type IV isotherms with H3 hysteresis loop shape, which indicates that all are mesoporous materials with good degree of order (Sing & Williams, 2004). Pore size distribution shows that these materials have an average pore diameter ranging from 5.35 nm to 5.86 nm. As presented in Table 1, it was apparent that there was a reduction in the specific surface area as compared to bulk alumina (S_{BET} = 138 m^2/g). This could be explained due to partial pore plugging. In addition, the incorporation of catalysts reduced the pore diameter, as the presence of nanoparticles diffused into the porosities resulting in a thinner pore (Movasati et al., 2019). This suggests that MOF-derived catalysts deposit inside the pore of the alumina supporter. Furthermore, it was apparent that the specific surface area of the catalyst decreased after the activity test, explaining the blockage of hollow mesopores due to carbon deposition (Das et al., 2018).
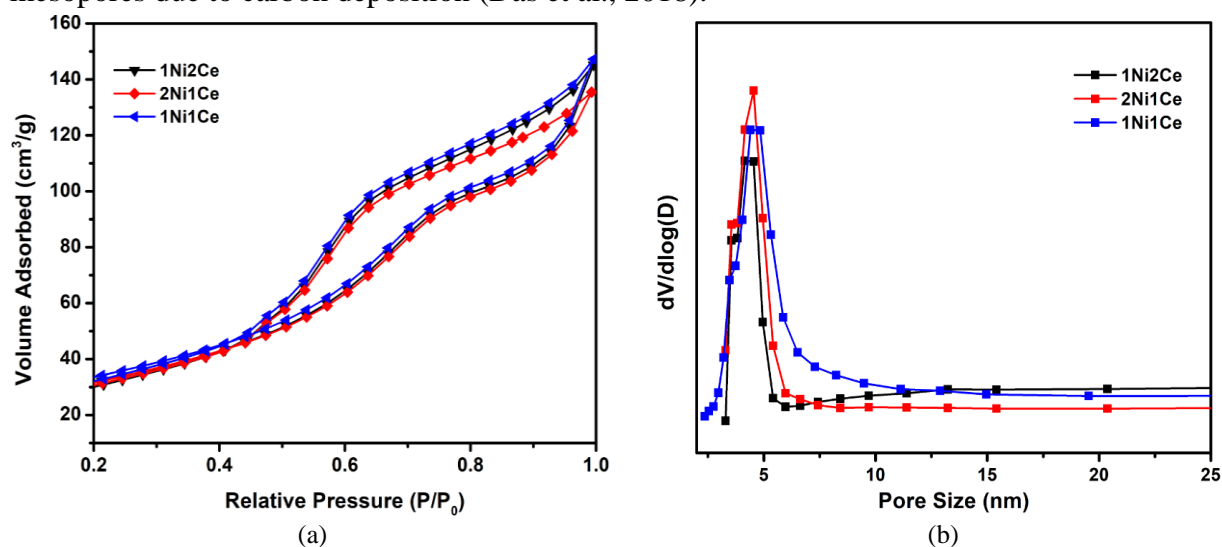

(a)   (b)

Figure 2 (a) N$_2$ adsorption–desorption isotherm; (b) Pore size distribution of supported MOF derived fresh catalyst

Table 1 Specific surface area and average pore diameter of MOF-derived catalyst

Catalyst	Specific Surface Area, S_{BET} (m²/g)		Average pore diameter (nm)	
	Fresh	Spent	Fresh	Spent
1Ni1Ce	104.34	75.60	5.36	4.72
2Ni1Ce	115.55	76.91	5.86	4.80
1Ni2Ce	114.92	68.50	5.35	4.68

The Ni crystallite size after reduction for all catalyst samples is presented in Table 2. As presented, the addition of CeO_2 promoted smaller particle size of Ni, ranging from 4.6 nm to 6.88 nm, which were relatively smaller size as compared to other preparation methods (Daza et al., 2009; Calles et al., 2015; Tan et al., 2017). It was observable that the Ni crystallite size decreased gradually with an increase in Ce content. This trend aligns with outcomes reported in literature, in which the implication of CeO_2 reduces Ni crystallite size, leading to a stronger dispersion of catalyst support (Tan et al., 2016).

ICP-OES and EDX analyses indicate that the weight percent of bimetallic metal of Ni and Ce was consistent as shown in Table 2, in which the amount of respective metal obeyed the ratio trend of the metal precursors added during the MOF synthesis. This also suggests the homogeneity of the catalyst, even though EDX showed relatively higher weight percent than ICP-OES. This could be explained that EDX focuses on surface composition analysis, hence the occurrence of surface metal enrichment shows higher weight percent as compared to ICP-OES, which involves the bulk composition of catalysts.

Table 2 Ni crystallite size ($2\theta = 44.5°$) (d_{Ni}), elemental composition of Ni and Ce from ICP-OES and EDX

Catalyst	d_{Ni} (nm)	Elemental Composition from ICP-OES		Elemental Composition from EDX	
		Ni (wt%)	Ce (wt%)	Ni (wt%)	Ce (wt%)
1Ni1Ce	5.54	4.98	0.11	13.29	5.38
2Ni1Ce	6.88	9.05	0.09	17.24	2.68
1Ni2Ce	4.60	7.96	0.27	10.99	7.06

Figure 3a shows the H_2-TPR profile of the MOF-derived catalyst with different bimetallic molar ratios. The predominant peak was observed at ~490°C for all samples, which was ascribed to the reduction of NiO species with weak interaction to the support (Daza et al., 2009). Even though reduction temperature showed no discernible change with Ce content, 2Ni1Ce showed a relatively lower reduction temperature at 489°C. In addition, the absence of a reduction peak at ~400°C due to amorphous NiO species suggests high degree and uniform dispersion of NiO_X species with the same coordination on catalyst support (Tan et al., 2016). This further supports the implication of the MOF precursor in producing highly-dispersed metallic particles. A reduction peak at 815°C was reported for 1Ni2Ce. This explains that at higher Ce molar loading, the reduction of bulk oxygen from CeO_2 to Ce_2O_3 in the crystalline network is initiated, supported by a reduction peak in the range of 800–840°C (Daza et al., 2009)

Due to the acidic nature of CO_2, CO_2-TPD was carried out in order to study the basicity of the catalyst as shown in Figure 3b. It was apparent from TPD profile that all catalysts showed at two CO_2 desorption peaks. First peak is explained as CO_2 adsorbed on weak basic sites at low temperature (50–200°C), while the latter predominated peak is CO_2 adsorbed on strong basic sites at higher temperature (500–650°C) (Pino et al., 2011). Moreover, the total amount of desorbed CO_2 was noticeably influenced by the introduction of Ce. The TPD profile shows that

an increase in Ce molar loading favoured strong basicity, in agreement with reported literature (Świrk et al., 2019). The basicity of the catalyst was arranged in the following order: 1Ni2Ce > 1Ni1Ce > 1Ni2Ce.
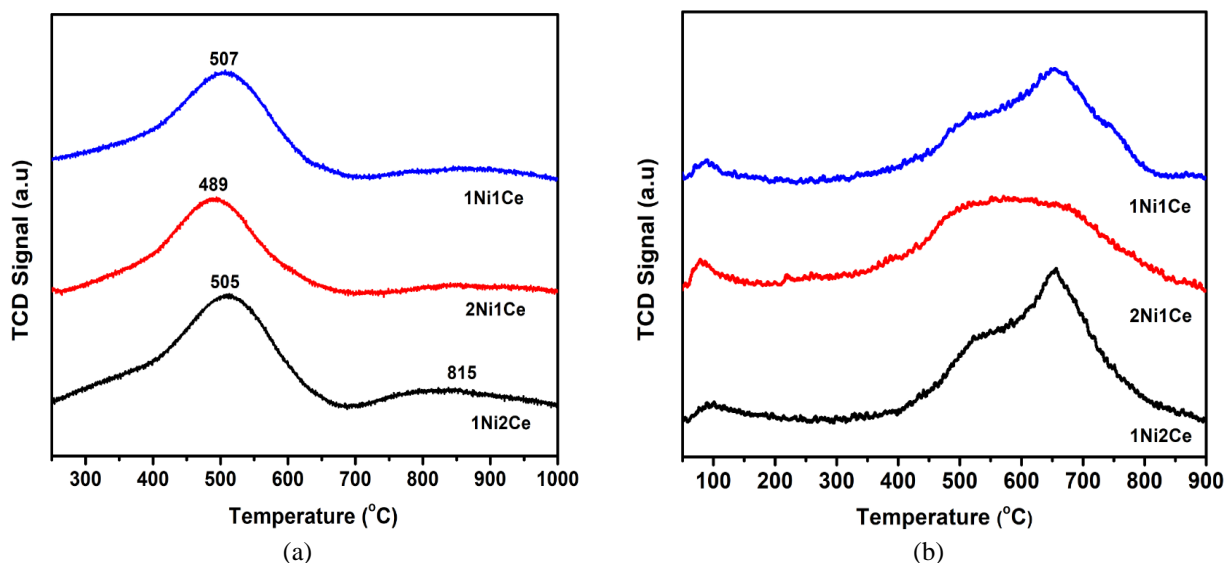

Figure 3 (a) H_2-TPR profile; and (b) CO_2-TPD of supported MOF derived catalyst

3.2. Catalytic Performance Evaluation

Figure 4 shows the conversion of CH_4 and CO_2 as function of temperature for each catalyst, in dry reforming of CH_4 on the promoted catalyst with a varying molar ratio of Ni:Ce. Satisfying the H_2-TPR profile, no observable catalytic activity was shown between 300–450°C for all catalysts because Ni species was not reduced at this temperature range. Additionally, the catalyst showed activity at relatively lower temperature for 2Ni1Ce, in agreement with relatively lower reduction temperature under similar characterization. As shown in the figure, CH_4 and CO_2 conversion for all catalysts increased from 500 to 800°C. Among the catalyst, the catalyst with greatest content of Ce (1Ni2Ce) registered stronger performance, showing CH_4 and CO_2 conversion at 63.5% and 86.8%, respectively at 800°C. This trend was in accordance with XRD and CO_2-TPD, in which the introduction of Ce improved the catalytic performance by enhancing smaller crystallite size of Ni in active phase, as well as providing more basic sites. In addition, for 2Ni1Ce the catalyst showed comparable activity between 450–700°C, with CH_4 and CO_2 conversion at 58.3% and 69.1%, respectively at 700°C. However, the catalytic conversion deteriorated significantly for both CH_4 and CO_2 at temperature of 750°C and above, suggesting a sintering effect due to large crystallite size as shown in XRD.

In order to further examine the influences of Ce promotion, isothermal tests were performed at 800°C for 7 hours, as shown in Figure 5 for all catalysts. No appreciable deactivation was observed for 1Ni2Ce. However, both CH_4 and CO_2 conversion experienced a significant decrease of 20.9% and 22.93%, respectively for 2Ni1Ce. This was in accordance with the fact that the addition of Ce species promotes active Ni dispersion (Świrk et al., 2019). At higher Ce loading, sintering effect on active Ni could be significantly decreased due to greater Ni dispersion on supporter, resulting minimal deactivation on the CH_4 and CO_2 conversions.
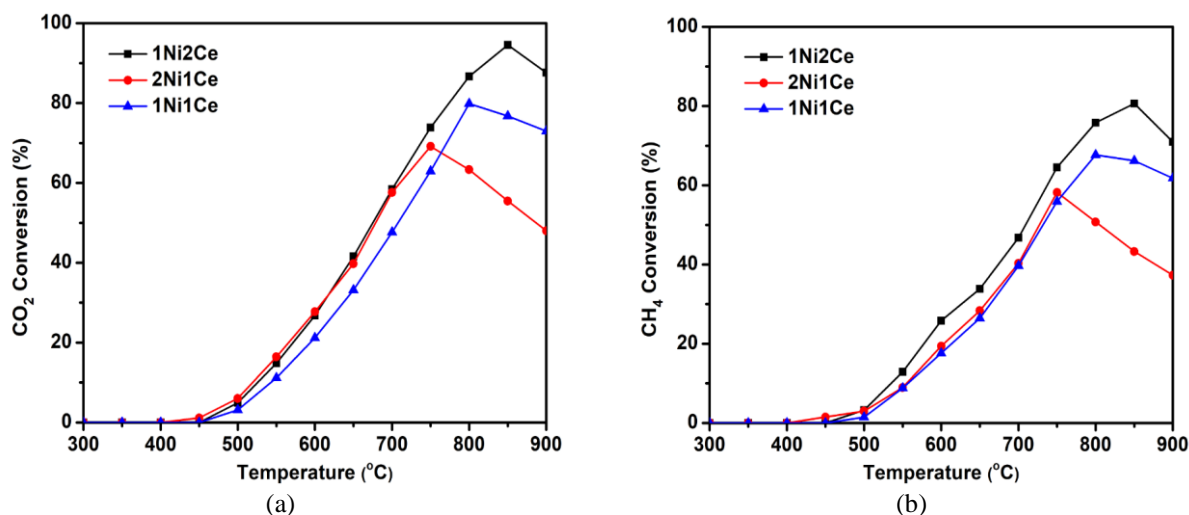
Figure 4 Catalytic: (a) CO_2; and (b) CH_4 conversion of supported MOF derived catalyst as function of temperature
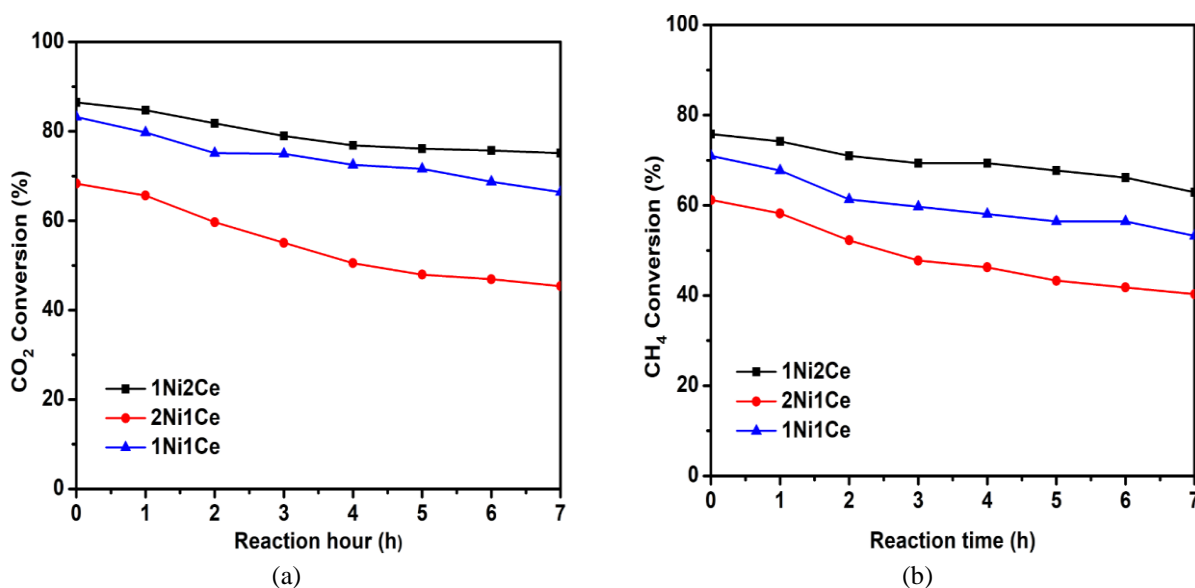

Figure 5 Stability: (a) CO_2; and (b) CH_4 conversion of supported MOF derived catalyst as function of reaction time for 7 h

4. CONCLUSION

MOF-derived catalysts prepared by solvothermal method exhibited convincing results for the design of a performing catalyst for the DRM process. The results from TPR justify the utilization of MOF as a precursor to produce highly-dispersed metallic particles. In addition, the promotion of Ce showed significant influence on the catalytic performance of the Ni-based catalyst. Increasing Ce molar loading enhanced a smaller Ni cluster size and provided more basic sites, in agreement with XRD and CO_2-TPD characterisation, respectively. The addition of Ce did not show a significant change in the reduction temperature of Ni active phase. However, the reduction of bulk oxygen from CeO_2 was observed at higher Ce loading. Within the range of the studied molar ratios, 1Ni2Ce showed the highest CH_4 and CO_2 conversion at 63.5% and 86.8%, respectively at 800°C, as well as greater stability within a 7-hour time frame, further supporting the promotion of Ce.

5. ACKNOWLEDGEMENT

6. REFERENCES

Anderson, T.R., Hawkins, E., Jones, P.D., 2016. CO_2, The Greenhouse Effect and Global Warming: From the Pioneering Work of Arrhenius and Callendar to Today's Earth System Models. *Endeavour*, Volume 40(3), pp. 178–187

Calles, A.J., Carrero, A., Vizcaíno, J.A., Lindo, M., 2015. Effect of Ce and Zr Addition to Ni/SiO_2 Catalysts for Hydrogen Production through Ethanol Steam Reforming. *Catalysts,* Volume 5(1), pp. 58–76

Das, S., Sengupta, M., Bag, A., Shah, M., Bordoloi, A., 2018. Facile Synthesis of Highly Disperse Ni–Co Nanoparticles over Mesoporous Silica for Enhanced Methane Dry Reforming. *Nanoscale*, Volume 10(14), pp. 6409–6425

Daza, C.E., Kiennemann, A., Moreno, S., Molina, R., 2009. Dry Reforming of Methane using Ni–Ce Catalysts Supported on a Modified Mineral Clay. *Applied Catalysis A: General*, Volume 364(1–2), pp. 65–74

Kim, W.Y., Lee, Y.H., Park, H., Choi, Y.H., Lee, M.H., Lee, J.S., 2016. Coke tolerance of Ni/Al_2O_3 Nanosheet Catalyst for Dry Reforming of Methane. *Catalysis Science & Technology*, Volume 6(7), pp. 2060–2064

Loc, L.C., Phuong, P.H., Tri, N., 2017. Role of CeO_2 Promoter in NiO/α-Al_2O_3 Catalyst for Dry Reforming of Methane. *In:* AIP Conference Proceedings, Volume 1878(1), pp. 20033

Nataj, S.M.M., Alavi, S.M., Mazloom, G., 2019. Catalytic Performance of Ni supported on ZnO-Al_2O_3 Composites with Different Zn Content in Methane Dry Reforming. *Journal of Chemical Technology Biotechnology*, Volume 94(4), pp. 1305–1314

Movasati, A., Alavi, S.M., Mazloom, G., 2017. CO_2 Reforming of Methane over Ni/$ZnAl_2O_4$ Catalysts: Influence of Ce Addition on Activity and Stability. *International Journal of Hydrogen Energy*, Volume 42(26), pp. 16436–16448

Movasati, A., Alavi, S.M., Mazloom, G., 2019. Dry Reforming of Methane Over CeO_2-$ZnAl_2O_4$ Supported Ni and Ni-Co Nano-catalysts. *Fuel*, Volume 236, pp. 1254–1262

Pakhare, D., Spivey, J., 2014. A Review of Dry (CO_2) Reforming of Methane over Noble Metal Catalysts. *Chemical Society Reviews*, Volume 43(22), pp. 7813–7837

Pino, L., Vita, A., Cipitì, F., Laganà, M., Recupero, V., 2011. Hydrogen Production by Methane Tri-reforming Process over Ni–ceria Catalysts: Effect of La-doping. *Applied Catalysis B: Environmental*, Volume 104(1–2), pp. 64–73

Rogge, S.M.J., Bavykina, A., Hajek, J., Garcia, H., Olivos-Suarez, A.I., Sepúlveda-Escribano, A., Vimont, A., Clet, G., Bazin, P., Daturi, M., Ramos-Fernandez, E.V., Xamena, F.X.L., Spreybroeck, V.V., Gascon, J., 2017. Metal–organic and Covalent Organic Frameworks as Single-Site Catalysts. *Chemical Society Reviews*, Volume 46(11), pp. 3134–3184

Rubin, E.S., Davison, J.E., Herzog, H.J., 2015. The Cost of CO_2 Capture and Storage. *International Journal of Greenhouse Gas Control*, Volume 40, pp. 378–400

San-José-Alonso, D., Juan-Juan, J., Illán-Gómez, M.J., Román-Martínez, M.C., 2009. Ni, Co and Bimetallic Ni–Co Catalysts for the Dry Reforming of Methane. *Applied Catalysis A: General*, Volume 371(1–2), pp. 54–59

Senthil Raja, D., Chuah, X.F., Lu, S.Y., 2018. In Situ Grown Bimetallic MOF-based Composite as Highly Efficient Bifunctional Electrocatalyst for Overall Water Splitting with Ultrastability at High Current Densities. *Advanced Energy Materials*, Volume 8(23), pp. 1801065

Sing, K., Williams, R., 2004. Physisorption Hysteresis Loops and the Characterization of Nanoporous Materials. *Adsorption Science and Technology*, Volume 22(10), pp. 773–782

Smith, K.R., Desai, M.A., Rogers, J.V, Houghton, R.A., 2013. Joint CO_2 and CH_4 Accountability for Global Warming. *In:* Proceedings of the National Academy of Sciences, Volume 110(31), pp. E2865 LP-E2874

Solomon, G., Nwaokocha, C., Ogunbona, C., Shittu, O., 2017. Hydrogen Production from Alternative Aqueous Sources: A Feasibility Study. *International Journal of Technology*, Volume 8(5), pp. 867–877

Souza, M.d.M.V., Clavé, L., Dubois, V., Perez, C.A., Schmal, M., Figueroa, J.D., 2004. Activation of Supported Nickel Catalysts for Carbon Dioxide Reforming of Methane. *Applied Catalysis A: General*, Volume 272(1–2), pp. 133–139

Świrk, K., Rønning, M., Motak, M., Beaunier, P., Da Costa, P., Grzybek, T., 2019. Ce- and Y-Modified Double-layered Hydroxides as Catalysts for Dry Reforming of Methane: On the Effect of Yttrium Promotion. *Catalysts*, Volume 9(56), pp. 1–18

Tan, J.S., Danh, H.T., Singh, S., Truong, Q.D., Setiabudi, H.D., Vo, D.-V.N., 2017. Syngas Production from CO_2 Reforming and CO_2-steam Reforming of Methane Over Ni/Ce-SBA-15 Catalyst. *IOP Conference Series: Materials Science and Engineering*, Volume 206(conference 1), pp. 1–13

Tan, M., Wang, X., Huang, H., Chen, C., Zou, X., Ding, W., Lu, X., 2016. Preparation of Cerium-Doped Mesoporous γ-Alumina Supported Nickel Catalysts for Pre–reforming of Liquefied Petroleum Gas under Low Steam to Carbon Ratio. *Chemistry Select*, Volume 1(8), pp. 1580–1587

Tristantini D., Supramono, D., Suwignjo, R.K., 2015. Catalytic Effect of K_2CO_3 in Steam Gasification of Lignite Char on Mole Ratio of H_2/CO in Syngas. *International Journal of Technology*, Volume 6(1), pp. 22–30

Winanti, W., Purwanto, W., Bismo, S., 2014. Decomposition of Carbon Dioxide in the Three-Pass Flow Dielectric Barrier Discharge Plasma Reactor. *International Journal of Technology*, Volume 5(1), pp. 1–11